Physical properties of meteorites – applications in space missions to asteroids

T. Kohout[1, 2, 3,*], G. Kletetschka[3, 4,5], T. Elbra[1], T. Adachi[4,5],V. Mikula[4,5], L. J. Pesonen[1], P. Schnabl[2, 3], S. Slechta[2, 3]

1. Department of Physics, University of Helsinki, P. O. Box 64, 00014, Helsinki University, Finland. tomas.kohout@helsinki.fi
2. Department of Applied Geophysics, Charles University in Prague, Prague, Czech Republic
3. Institute of Geology, Academy of Sciences, Prague, Czech Republic
4. Department of Physics, Catholic University of America, Washington D.C., USA
5. GSFC/NASA; Code 691, Greenbelt, MD, USA

* Corresponding author

Key words

asteroid; meteorite; physical properties; magnetic susceptibility; induced magnetization, remote sensing; density; solar wind, IMF.

Abstract

Based on reflectance spectroscopy and chemical / mineralogical remote sensing methods it is generally assumed that asteroids are parent bodies for most meteorites reaching the Earth. However, more detailed observations indicate that differences exist in composition between asteroids and meteorites resulting in difficulties when searching for meteorite – asteroid match.

We show that among other physical parameters the magnetic susceptibility of an asteroid can be determined remotely from the magnetic induction by solar wind using an orbiting spacecraft or directly using the AC coil on the lander or measured on sample return in the laboratory. The shape corrected value of the true magnetic susceptibility of an asteroid can be compared to those of meteorites in the existing database allowing closer match between asteroids and meteorites. The database of physical properties contains over 700 samples and was recently enlarged with measurements of meteorites in European museums using mobile laboratory facility.

Introduction

The objective of asteroid and comet investigation is the characterization and classification of these bodies using remote data acquisition systems. It is generally assumed that asteroids are parent bodies for most

meteorites reaching the Earth (Wasson and Wetherill, 1979; Feirberg et al, 1982). The reflectance spectroscopy of asteroids proved to be powerful tool in characterization of the asteroid composition and classification. The extended taxonomy (Tholen, 1984; modified by Bus and Binzel, 2002) defines total of 26 classes of the asteroid reflectance spectra. Three major groupings (S, C, and X complexes) show spectral similarities to the major meteorite groups. The composition of the S-class asteroids is similar to the silicate-rich ordinary chondrite group, the C-class contains asteroids which are rich in carbonaceous material similar to that of carbonaceous chondrite group and X-class contains various asteroid types mostly rich in metallic component. However, when analyzing the whole spectral curve the exact match between asteroids and meteorites is not found due to differences in their spectral patterns.

Thus, other remote sensing methods are applied during asteroid reconnaissance in order to improve the knowledge of the asteroid chemical and mineralogical composition and to determine possible meteorite equivalents to the asteroid compositions. We show that the physical properties of asteroids and meteorites – mainly the magnetic susceptibility and density – can be applied along with the chemical and mineralogical methods in building the link between meteorites and asteroids.

Instruments and methods

The meteorites represent valuable rare material and it is difficult to bring meteorites directly to the laboratory for scientific studies. Thus, the mobile laboratory facility including portable instrumentation was assembled at Division of Geophysics, University of Helsinki in order to perform the research tour over the museums and collections in Europe and to measure the physical properties of meteorites using harmless, non-destructive methods.

During the meteorite research tour the measurements of bulk physical parameters (magnetic susceptibility, bulk and grain density and porosity) of meteorites were performed. Due to the rare nature of meteorites only harmless, non-destructive methods were applied.

The Hämäläinen TH-1 portable susceptibility meter with large (12 cm) coil was used for susceptibility measurements of bulk samples and was cross-calibrated with the laboratory RISTO 5 and Agico KLY-3 susceptibility meters.

In order to determine the meteorite bulk and grain density as well as porosity the bulk and grain volume and mass must be measured. For bulk volume measurements the chemically inert tiny glass beads (20 – 50 μm) were used to replace liquids used in traditional Archimedean method. The precision of the glass beads method is ±0.1 cm^3. The mass was determined using digital OHAUS balances. The balances were always calibrated prior the measurements using mass standards.

The grain volume was measured by Notari portable air pycnometer working at low pressures. The advantage of this instrument is that it does not require any supply gas and thus is easy to transport. The precision of the pycnometer is ±0.1 cm^3.

The instruments can be easily fitted in a small van building a mobile meteorite laboratory (Kohout *et al.*, 2006). This approach enables to perform the meteorite physical properties measurements using non-destructive methods directly in the meteorite collections under the supervision of the curator.

Figs. 1 and 2 compare the data obtained in the museums using mobile meteorite laboratory (colored symbols) with the older data obtained using fixed laboratory instrumentation (grey symbols). The good agreement between those two data sets proves a good cross-calibration between the portable and laboratory instrumentations.

Magnetic susceptibility of stony meteorites

Magnetic susceptibility of various meteorites has been systematically studied by Kukkonen and Pesonen, 1983; Terho *et al.*, 1993a, 1993b; Rochette *et al.*, 2001, 2003, 2008; Kohout *et al.*; 2006. The results of these studies indicate that the magnetic susceptibility of various meteorite clans and groups occupy characteristic values with quite uniform distribution (Fig. 1). According to those studies the lowest susceptibility is occupied by SNC (10-100 10^{-8} m^3/kg) and HED (10-1000 10^{-8} m^3/kg) achondrites. Aubrites have also low susceptibility values (400-3000 10^{-8} m^3/kg). Chondrite clan has higher susceptibilities in range of 4000-80000 10^{-8} m^3/kg (with exception of R-chondrites occupying range of 100-160 10^{-8} m^3/kg) and stony-irons and irons occupy the highest susceptibility range (100000-2000000 10^{-8} m^3/kg). However, it is difficult to measure the true magnetic susceptibility of stony-irons and irons due to the shape effect (see section "The role of shape and demagnetization factor") and thus the values contain high level of uncertainty.

The iron content of undifferentiated meteorites is both within the silicates and in the form of fine magnetic grains. Magnetic properties of ordinary chondrite clan (Wasilewski *et al.*, 2002) are mostly related to Fe-Ni compounds, namely α-kamacite (<7% Ni), γ-taenite (>7% Ni), and γ"-tetrataenite (43-52% Ni) capable of carrying remanent magnetization (Morden and Collinson, 1992; Wasilewski, 1988). The susceptibility of the ordinary chondrites (Fig. 2) is directly related to the amount of metal (FeNi) fraction in non-oxidized form. The lowest susceptibility values occupy the LL chondrite group with range of approximately 300-4000 10^{-8} m^3/kg followed by L chondrite group (4000-14000 10^{-8} m^3/kg) and H chondrite group (14000-46000 10^{-8} m^3/kg). The susceptibility of enstatite chondrite clan falls mostly in range of 46000-80000 10^{-8} m^3/kg. Urelites occupy similar susceptibility range (6000-15000 10^{-8} m^3/kg) as L type chondrites.

The magneto-mineralogy of the carbonaceous chondrite clan (Rochette *et al.*, 2008) is more complicated containing not only the FeNi, but also oxides, sulphides and carbides. The CM, CV and C2 groups occupy roughly the range of 400-4000 10^{-8} m^3/kg while the CO3, CK and CI groups fall mostly in the range of 2500-6300 10^{-8} m^3/kg. The C3-4 groups are characterized by susceptibilities in range of 3100-10000 10^{-8} m^3/kg. The CR group has values around 10000 10^{-8} m^3/kg. The highest susceptibility values among carbonaceous chondrites (comparable to those of enstatite chondrite clan) occupy CH group with range of 16000-63000 10^{-8} m^3/kg. The magnetic susceptibilities of various carbonaceous chondrite groups overlap and are similar to those of ordinary chondrites. However, comparing to ordinary chondrites, the carbonaceous chondrites have in general lower bulk and grain densities (Consolmagno and Britt, 1998; Britt and Consolmagno, 2003; Wilkinson *et al.*, 2003).

The Finnish database of physical properties of meteorites

The research work of Kukkonen and Pesonen, 1983; Terho *et al.*, 1993a, 1993b and Kohout *et al.*, 2006 has been has been merged in a form of database counting measurements of more than 700 individual meteorite samples from European meteorite collections and is continuously expanded. The database contains measurements of physical parameters including bulk (volume normalized) and mass susceptibility, bulk and grain density, porosity, NRM (Natural Remanent Magnetization), Q-value (Königsberger ratio), various hysteresis parameters and magnetic paleointensity estimates.

In table 1 we present new unpublished mass normalized as well as volume normalized shape corrected magnetic susceptibility values, bulk and grain densities and porosities of meteorite samples obtained using the mobile laboratory (colored symbols in Figs. 1 and 2).

The role of the shape and demagnetization factor

The magnetic susceptibility κ of the body determined in the ambient magnetic field B is influenced by the shape and dimensions of the body. Thus the measured (apparent) magnetic susceptibility κ_A should be corrected for this shape effect in order to get the shape independent true susceptibility κ_T. The true susceptibility as a shape independent parameter can be used as a comparative parameter between meteorites and asteroids.

The relation between the true and apparent volume susceptibility is characterized by the equations (1, 2):

$$\kappa_T = \frac{\kappa_A}{1 - N\kappa_A} \qquad (1)$$

or

$$\kappa_A = \frac{\kappa_T}{1 + N\kappa_T} \qquad (2)$$

where N is the demagnetizing factor. The demagnetizing factor is depending on the shape of the object and direction along which the magnetic susceptibility is determined. For ellipsoid-shaped bodies the demagnetization factor can be calculated along the ellipsoid axes using the approach of Osborn, 1945.

In table 2 the shape effect has been determined for the rotational ellipsoids with various a to b,c axis ratios and for the susceptibilities ranging from 500 to 500000 10^{-8} m^3/kg (0,016 to 16 SI, assuming density of 3200 kg/m^3). It is apparent that at the susceptibility values ~0,1 SI the difference between κ_A and κ_T for elongated objects can reach more than 10 %. At even higher susceptibility values this difference is more pronounced and for values $\kappa_T >> 1$ SI the equation (2) reach the form (3)

$$\kappa_A \approx \frac{1}{N} \qquad (3)$$

This condition is met for iron and stony-iron meteorites and thus the apparent susceptibility κ_A is strongly controlled by the shape of the body and the true susceptibility value κ_T contains large uncertainty resulting in large scatter of the true susceptibility values (see figure 1).

All the meteorite susceptibility values presented in the figures 1 and 2 are corrected for the shape of the sample.

Determination of asteroidal magnetic susceptibility

Knowledge of asteroidal magnetic susceptibility could help to identify the metallic nature of the asteroid interior without direct access. However, the determination of this parameter is not easy task. Magnetic susceptibility of the asteroid may be detected in three ways with various levels of uncertainty:

1. Passively from an induced magnetization by interplanetary magnetic field (IMF).
2. Actively using a surface probe (AC coil) attached to a lander.
3. Directly on a sample return from asteroid.

1. Remote determination of the asteroidal magnetic susceptibility from induced magnetization by interplanetary magnetic field

The interplanetary magnetic field (IMF) is carried through Solar System in the solar wind. When encountering the asteroid the IMF gets disturbed. The level of this interaction depends on the magnetic properties of the asteroid. The asteroids with low remanent magnetization and low magnetic susceptibility will cause minor distortion while the asteroids with high remanent magnetization and / or high magnetic susceptibility can cause high disturbances in the IMF.

Those interactions can be measured using an orbiting spacecraft equipped with a magnetometer. In the case of significant interactions between asteroid and IMF have been detected first task is to separate the interactions due to the remanent magnetization from those due to the induced effect. Only the induced magnetization contains the information about the magnetic susceptibility. The basic criteria used to separate the remanent and induced magnetization are the facts that remanent magnetization of an asteroid has a stable value and direction and thus rotates with the asteroid while the induced (by the IMF) magnetization has always the direction of the IMF and its magnitude correlates positively with the magnitude of the IMF (and with the magnetic susceptibility of the asteroid). The remanent magnetization of an asteroid can be also easily determined in the periods of low IMF magnitudes when the induced effects are negligible.

Once the remanent magnetic field of an asteroid is well determined or is proved that the asteroid has negligible remanence the induced magnetic field during the periods of the high IMF magnitudes can be used to determine the magnetic susceptibility (unpublished data, Kletetschka *et al*., 2007).

The separation of the induced magnetic measurements according to the dipole rules will generate data sets containing induced magnetization that allow an estimate of magnetic susceptibility. However, the solar wind interaction with the surface is a complex process and has to be considered during such estimate of magnetic susceptibility (Omidi et al., 2002). In the case the plasma carrying the external magnetic field H is homogenous during the measurement period (couple of orbits), the resulting magnetic induction B measured on orbit of the asteroid is:

$$\begin{aligned} B &= \mu H \\ B &= \mu_0 \mu_r H \\ B &= \mu_0 (1+\kappa) H \\ B &= \mu_0 H + \mu_0 \kappa H \\ B &= \mu_0 (H + M) \\ B &= B_s + B_a \end{aligned} \qquad (4)$$

where μ is permeability, μ_0 is permeability of vacuum, μ_r is relative permeability, κ is volume normalized magnetic susceptibility, M is magnetization induced by H, B_s is an induction from the Sun and B_a is an induction from the asteroid.

B_a propagates as magnetic dipolar field according to:

$$B_a = \frac{\mu_0}{4\pi} \frac{m}{r^3} \sqrt{1 + 3\sin^2 \alpha}, \qquad (5)$$

where m is a magnetic moment of the asteroid, r is a distance form the center of the asteroid, and α is the magnetic latitude of the dipole.

Dipole equation (5) can be detected as the difference between the asteroid induction $B_a(90°) = \frac{\mu_0}{2\pi}\frac{m}{r^3}$ over the magnetic pole (Case A in Figure 3) and asteroid induction $B_a(0°) = -\frac{\mu_0}{4\pi}\frac{m}{r^3}$ over the magnetic equator (Case B in Figure 3, note the negative sign reflecting the opposing direction in respect to inducing field B_s).

This difference due to dipolar character of the induced field suggests a scheme for detection of an induced component on board of the spacecraft. The data has to be transformed into a coordinate system such that the vertical direction is parallel to spacecraft-asteroid direction. If the magnetic field B_A is parallel to spacecraft-asteroid direction, we have the case A in Figure 3. If the magnetic field B_B is perpendicular, we have the case B in Figure 3. The difference between these two cases δB can be expressed as following:

$$\begin{aligned}
\delta B &= B_A - B_B \\
\delta B &= B_s + B_a(90°) - B_s - B_a(0°) \\
\delta B &= B_a(90°) - B_a(0°) \\
\delta B &= \frac{\mu_0}{2\pi}\frac{m}{r^3} + \frac{\mu_0}{4\pi}\frac{m}{r^3} \\
\delta B &= \frac{3\mu_0}{4\pi}\frac{m}{r^3}
\end{aligned} \qquad (6)$$

where m is the magnetic moment for which we have:

$$\begin{aligned}
m &= MV_a \\
m &= \kappa H V_a
\end{aligned} \qquad (7)$$

where M is asteroid's magnetization, κ is bulk susceptibility (asteroid volume (V_a) normalized) and H is magnetic field, so we have:

$$\begin{aligned}
\delta B &= \frac{3\mu_0}{4\pi}\frac{\kappa H}{r^3}V_a \\
\delta B &= \frac{3}{4\pi r^3}\kappa V_a B_s
\end{aligned} \quad . \qquad (8)$$

where B_s is the solar induction. Equation (8) allows detection of susceptibility of the entire asteroid from any data set satisfying the case A and B (Figure 3). For B_s we can use an average from values B_A and B_B:

$$B_{av} = \frac{B_A + B_B}{2}$$

$$B_{av} = B_s + \frac{B_a(90°) + B_a(0°)}{2}$$

$$B_{av} = B_s + \frac{\mu_0}{4\pi}\frac{m}{r^3}$$

$$B_{av} = B_s + \frac{\mu_0 H}{4\pi r^3}\kappa V_a \qquad (9)$$

$$B_{av} = B_s + \frac{B_s}{4\pi r^3}\kappa V_a$$

$$B_{av} = B_s\left(1 + \frac{\kappa V_a}{4\pi r^3}\right)$$

$$B_{av} \sim B_s$$

because the term $\frac{\kappa V_a}{4\pi r^3} = \kappa\frac{V_a}{3V_r} < \kappa\frac{1}{100} << 1$ for $r > 1.5\ r_a$ (radius of an asteroid) and susceptibility κ even ≤ 1.

Finally we obtain:

$$\kappa = \frac{8\pi r^3}{3V_a}\frac{\delta B}{(B_A + B_B)} \qquad (10)$$

This formulation (10) can be used to estimate the apparent bulk susceptibility κ_{bulk} of an asteroid.

The advantage of this method is that the magnetic susceptibility of the whole asteroid is determined. This gives us the susceptibility value representative for the whole asteroidal volume and free of surface related space weathering affects. However, comparing to the surface or sample return measurements the sensitivity and precision of this method is low.

Usual IMF in the asteroid belt is about in the order of nT but can reach larger amplitudes during the periods of the high solar activity giving better signal to noise ratio. The induced magnetic field decays with power of three of the distance from the asteroid thus requiring close orbits.

The detection limit and desired magnetometer sensitivity depends on two main factors – the strength of the IMF field and the orbiting distance. In order to estimate the detection limit we will use in our calculation a spherical asteroid, radius of the orbit twice large than the radius of the asteroid $r = 2r_a$ (in order to meet the condition in equation (9)) and IMF strength 10 nT. Then, by using the approximation from equation (9):

$$B_s \sim B_{av} = \frac{B_A + B_B}{2}$$

and

$$V_a = \frac{4}{3}\pi r_a^3$$

the equation 10 will transfer to

$$\kappa = \frac{r^3}{r_a^3}\frac{2\delta B}{B_s} = \frac{8r_a^3}{r_a^3}\frac{2\delta B}{B_s} = \frac{16\delta B}{B_s} \qquad (11)$$

For asteroid with CH, E or H composition equivalent (κ_{bulk} ~1 SI) and IMF strength 10 nT the measured variation due to the induced effect will be ~0.6 nT and for CR, H or Urelite composition equivalent (κ_{bulk} ~0.1 SI) the measured variation due to the induced effect will be ~0.6 nT.

Thus in the case of strongly magnetic stony asteroids or metallic objects the detection of magnetic susceptibility (and thus estimate of the iron content) is possible using currently available magnetometers with 10^{-1} nT - 10^{-2} nT resolution. In the case of stony asteroids with lower magnetic content development of more sensitive instrumentation or use of other method (as described further) is needed.

Other problem is related to the time variation of the IMF. This method assumes IMF to be constant through the measurement period. Thus the measurement must be performed during the relatively stable IMF periods or the second spacecraft far from an asteroid is required to monitor the variations of undisturbed IMF.

2. Active detection of asteroidal magnetic susceptibility using a surface probe (AC coil) attached to a lander

In the case asurface landing is the part of the asteroid space mission, a simple AC magnetic coil surface probe can be used for the magnetic susceptibility measurement. This concept is described in detail in Rochette *et al.*, 2004. The advantage of this method is that the signal of the material induced by the coil is much stronger comparing to the IMF interactions. The depth penetration of the coil signal depends on its diameter (roughly equal to the coil diameter) and usually the flat surface is required for best precision.

However, the effect of the space weathering on the magnetic properties of the asteroidal surface is not well known. In the case of a solid rocky surface of an asteroid the combination of the surface susceptibility probe with the device similar to RAT (Rock Abrasion Tool) used on Mars Exploration Rovers could provide the magnetic susceptibility of the unweathered asteroidal material. Other disadvantage is that the surface material of the asteroid can be modified or contaminated through collisional impact processes. Due to those reasons the magnetic susceptibility determined by the surface probe may not be representative for the whole asteroid.

3. Directly measurement of the asteroidal sample return

In the case the sample of the asteroid is delivered to the terrestrial laboratories the magnetic susceptibility can be measured using sensitive and well calibrated laboratory instrumentation. However, the expected sample size of the sample return for the ongoing (Hayabusa) or planned mission is typically very small (~mg) and may also be influenced by the effects described in the previous case. Thus, it may not be representative for the whole asteroid as well.

Mass vs. bulk susceptibility

The bulk volume V_B, mass m, bulk density ρ_B and shape are among the primary asteroid parameters determined during the orbital phase of the asteroid remote sensing mission. Knowledge of both bulk volume and mass of the asteroid enables determination of both bulk (volume normalized) and mass normalized susceptibility of the asteroid. The relation between mass and bulk susceptibilities is expressed by equation (11):

$$\kappa_{mass} = \frac{\kappa_{bulk}}{\rho_B} \tag{11}$$

The bulk susceptibility is essential to calculate the shape correction of the measured (apparent) susceptibility using the demagnetizing factor and equation (1). However the bulk volume V_B of the asteroid may vary according to the porosity of the asteroid. An asteroid of the same mass and grain volume V_G (and thus same amount of magnetic compounds), but higher pore volume V_P, will have larger bulk volume V_B resulting in the lower bulk susceptibility. Thus bulk susceptibility is not suitable for the magnetic classification purposes.

However, the mass m and grain volume V_G remains the same and thus susceptibility normalized by mass or by grain volume will remain independent on the change in porosity. For this reason it is suitable to first perform the shape correction of the apparent bulk susceptibility and then normalize the true bulk susceptibility by mass or grain volume in order to minimize the porosity effect. Then the mass (or grain volume normalized) true susceptibility can be directly compared to those of meteorites.

Conclusions

Determination of the asteroidal susceptibility is not a trivial task, but is possible. Each of three methods described has its own advantages and disadvantages. The induced effects due to the IMF interactions can provide the susceptibility representative for the whole asteroid. However the precision of this method is lower and thus is suitable for the high susceptible bodies only. The use of surface probe or the laboratory measurement of the sample return can provide more reliable values and can bring results also for

materials of lower susceptibility (e.g. achondrites). However, these methods bring the information from the asteroid surface only and thus does may not be representative for the whole asteroid.

Once magnetic susceptibility is successfully determined, the amount and nature of the magnetic minerals can be inferred. Based on the susceptibility, asteroids can be classified in similar way as meteorites are. We expect the distribution of magnetic susceptibility among various asteroid compositions to reflect the distribution of their meteorite equivalents. Similarly as for meteorites, the range of the susceptibilities of some asteroid classes may overlap. But additionally to reflectance spectroscopy and other chemical and mineralogical remote sensing methods, the magnetic classification may refine the match among meteorite equivalent candidates.

Thus we propose a stepwise concept of asteroid characterization and classification. First, the spectral class will be determined based on reflectance spectroscopy classification and the corresponding meteorite clan will be determined. In a second step, based on the asteroid magnetic susceptibility as well as on chemical and mineralogical information from the instruments on board of the space probe, the matching meteorite group will be distinguished. This multidisciplinary approach will help us to get the most precise link among asteroids and meteorites.

Once the meteorite equivalent will be distinguished, other physical parameters (bulk and grain density, porosity) of the asteroid and corresponding meteorite group in the database can be compared in order to determine more information about the internal structure asteroid. For example, by comparing the bulk and grain densities of the asteroids and meteorites, the amount of micro- and macro-porosity can be estimated. The micro-porosity is assumed to be similar among asteroids and related meteorites due to the small (sub-millimeter) pore size. This approach was applied in past studies to determine amount of the micro- and macro-porosity and the internal structure (rubble pile vs. onion skinned) of the asteroids Eros (Wilkinson *et al.*, 2000) and Itokawa (Abe *et al.*, 2006). The macro-porosity observed on asteroids is not preserved in meteorites because of the large-scale cracks / faults building the pore space. In this case the meteorites are simply too small to preserve those large scale cracks.

Acknowledgments

This work was financially supported by Academy of Finland project, Sohlberg Delegation research grant, NSF EAR-0609609, and Väisälän Foundation travel grant. We would like to thank V. Kohout for his help with the meteorite measurements and M. Lehtinen (Geological Museum, University of Helsinki, Finland), H. Pärnaste (Geological survey of Estonia, Tallinn), J. Plado (Tartu University, Estonia), B.Poshkiene (Geology and Mineralogy Museum, Vilnius, Lithuania), E. Rudnickaite and G. Motuza (Vilnius University, Lithuania), J. Biala and J. Szubiakowski (Planetarium and Observatory Olsztyn, Poland), O.

Kákay-Szabó (Geological Institute of Hungary, Budapest, Hungary), T. Weiszburg (Eötvös L. University, Budapest, Hungary), A. Embey-Isztin (Museum of Natural History, Budapest, Hungary), M. Bukovanská (National Museum, Prague, Czech Republic), A. Martaus and B. Kratochvíl (Chemical University, Prague, Czech Republic), A. Greshake (Humboldt University of Berlin, Germany), A. Bischoff (University of Münster, Germany), G. Raade (University of Oslo, Norway), J. O. Nyström (Swedish Museum of Natural History, Stockholm, Sweden) for cooperation and help in providing access to the meteorite collections.

References

Abe S., Mukai T., Hirata N., Barnouin-Jha O. S., Cheng A. F., Demura H., Gaskell R. W., Hashimoto T., Hiraoka K., Honda T., Kubota T., Matsuoka M., Mizuno T., Nakamura R., Scheeres D. J. and Yoshikawa M., 2006. Mass and local topography measurements of Itokawa by Hayabusa. Science, 312, 1344-1347.

Britt D. T. and Consolmagno G. J. Stony meteorite porosities and densities: A review of the data through 2001. Meteorites & Planetary Science 38, 1161-1180.

Bus S.J., Binzel R.P., 2002. Phase II of the Small Main-belt Asteroid Spectroscopic Survey - A feature-based taxonomy. Icarus 158, 146-177.

Consolmagno G. J. and Britt D. T. The density and porosity of meteorites from the Vatican collection. Meteorites & Planetary Science 33, 1231-1241., Nr 10, 1533-1546.

Kletetschka, G., Adachi, T., Mikula, V., Electromagnetic spacecraft used for magnetic navigation within asteroid belt, mining concepts and asteroid magnetic classification. 38th Lunar and Planetary Science Conference, Abstract #1093

Kohout T., Elbra T., Pesonen L. J., Schnabl P., Slechta S., 2006. Applications of the meteorite physical properties data obtained using mobile laboratory facility. Meteoritics & Planetary Science Supplement 41, A98.

Kukkonen I.T. and Pesonen L.J., 1983. Classification of meteorites by petrophysical methods. Bull. Geol. Soc. Finland 55, 2, 157-177.

Omidi N., X. Blanco-Cano, C. T. Russell, H. Karimabadi, and M. Acuna, 2002. Hybrid simulations of solar wind interaction with magnetized asteroids: General characteristics, J. Geophys. Res., 107 (A12), 1487, doi:10.1029/2002JA009441.

Osborn, J A., 1945. Demagnetizing factors of the general ellipsoid. Phys. Rev. 67, 351-357.

Rochette P., Gattacceca J., Bonal L., Bourot-Denise M., Chevrier V., Clerc J.-P., Consolmagno G., Folco L., Gounelle M., Kohout T., Pesonen L., Quirico E., Sagnotti L., Skripnik A., 2008. Magnetic Classification of Stony Meteorites: 2. Non-Ordinary Chondrites. Meteoritics & Planetary Science, in print.

Rochette P., Gattacceca J., Menvielle M., Eisenlohr P., Chevrier V., 2004. Interest and design of magnetic properties measurements on planetary and asteroidal landers. Planetary and Space Science, 52 (11). 987-995.

Rochette P., Sagnotti L., Bourot-Denise M., Consolmagno G., Folco L., Gattacceca J., Osete M. L., and Pesonen L., 2003. Magnetic classification of stony meteorites: 1. Ordinary chondrites. Meteoritics & Planetary Science 38, 251–268.

Rochette P., Sagnotti L., Consolmagno G., Folco L., Maras A., Panzarino F., Pesonen L., Serra R. and Terho M., 2001. A magnetic susceptibility database for stony meteorites. Quaderni di Geofisica 18, 30.

Terho M., Pesonen L.J. and Kukkonen I.T., 1993a. Physical properties of 368 meteorites: implications for meteorite magnetism and planetary geophysics. Proceedings of the NIPR Symposium on Antarctic Meteorites, 6, 601-416.

Terho M., Pesonen L.J., Kukkonen I.T. and Bukovanska M., 1993b. The petrophysical classification of meteorites. Studia Geophysica et Geodetica 37, 65-82.

Tholen D.J., 1984. Asteroid Taxonomy from Cluster Analysis of Photometry, University of Arizona (1984).

Wasilewski P. J., Acuna M. H. and Kletetschka G., 2002. 433 Eros: Problems with the meteorite magnetism record in attempting an asteroid match. Meteorites & Planetary Science, 37, 937-950.

Wasson, J.T. and Wetherill, G.W. in Asteroids, eds. T. Gehrels and M.S. Matthews (1979), U of Arizona Press, 926-974.

Wilkinson S. L., Robinson M. S., Thomas P. C., Veverka J., McCoy T. J., Murchie S. L., Prockter L. M. and Yeomans D., K., 2002. An estimate of Eros's porosity and implications for internal structure. Icarus 155, 94-103.

Wilkinson S. L., McCoy T. J., McCamant J. E., Robinson M. S., Britt D. T., 2003. Porosity and density of ordinaly chondrites: Clues to the formation of friable and porous ordinary chondrites. Meteorites & Planetary Science 38, 1533-1546.

Figure and table captions

Table 1: New mass normalized (KM) as well as volume normalized (KV) shape corrected magnetic susceptibility values, bulk (BD) and grain (GD) densities and porosities (P) of meteorite samples obtained using the mobile laboratory.

Legend to the collections and meteorite classes:
EUB - Eötvös. University, Budapest, Hungary
GMO - Geological Museum, Oslo, Norway
HMNHB - Hungarian Museum of Natural History, Budapest, Hungary
GSHB - Geological Survey of Hungary, Budapest, Hungary
HUB – Humboldt University, Berlin, Germany
IGGL - Institute. of Geology and Geography of Lithuania, Vilnius, Lithuania
NHMS – Natural History Museum, Stockholm, Sweden
PO - Planetarium Olsztyn, Poland
TIGT - Tallinn Institute of Geology, Tallinn, Estonia
TUT – Tartu University, Tartu, Estonia
UM - Planetary Institute, University of Münster, Münster, Germany
VUV – Vilnius University, Vilnius, Lithuania

ACA - Acapulconite
AEUC - Eucrite
AHOW – Howardite
AUB - Aubrites
AURE - Urelites
CX – Carbonaceous chondrites
H, L, LL – Ordinary chondrites
MES – Mesosiderites

Table 2: The shape effect has been determined for the rotational ellipsoids with various *a* to *b,c* axis ratios and for the susceptibilities ranging from 500 to 500000 10^{-8} m^3/kg (0,016 to 16 SI, assuming density of 3200 kg/m^3).

Figure 1: Magnetic susceptibility vs. bulk density of various meteorite clans. The lowest magnetic susceptibility values are characteristic to achondrites, followed by the chondrites, stony-irons and irons. The carbonaceous chondrite clan shows lowest bulk densities followed by other stony meteorites, stony-irons and iron meteorites. The grey symbols show older data obtained in laboratory while the colored symbols show new data measured directly in the museums using portable instruments. Only unweathered falls are displayed.

Figure 2: Magnetic susceptibility vs. bulk density of various ordinary chondrite groups and of enstatite chondrite clan. The magnetic susceptibility increases from LL chondrites to L, H and E chondrites. The grey symbols show older data obtained in laboratory while the colored symbols show new data measured directly in the museums using portable instruments. Only unweathered falls are displayed.

Figure 3:
Green and blue circles indicate magnetic orientations of the vector magnetic data during the orbiting of the asteroid. Background image (Eros asteroid) is shown just for concept visualization. A: Magnetic field directions (green circles) is directed towards the asteroid at the magnetometer location. B: Blue circles indicate magnetic vector directions of the magnetic field pointing 90 degrees away from the asteroid direction.

Table 1:

Meteorite	Collections	Type	Fall / Find (date)	mass (g)	BD (kg/m3)	GD (kg/m3)	P (%)	KM (Osb) (10^{-8} m^3/kg)	KV (Osb) (10^{-6} SI)
Juvinas	IGGL	AEUC	FA 15/06/1821	8.26	2503	3177	21		
Andrioniškio	VUV	AEUC	FA 1929	14.34	2988	3259	8		
Bereba	IGGL	AEUC	FA 27/06/1924	14.9	2811	3548	21		
Sioux County	IGGL	AEUC	FA 08/08/1933	20.41	3092	3519	12		
Bereba	VUV	AEUC	FA 27/06/1924	16.84	2903	3437	16		
Andrioniškio (Padvarninkai)	VUV	AEUC	FA 1929	119.7	3023				
Andrioniškio (Padvarninkai)	VUV	AEUC	FA 1929	104.1	3000				
Bialystok	HUB	AHOW	FA 05/10/1827	43.8	2607	3422	24		
Petersburg	TUT	AHOW	FA 05/08/1855	22.5	3261	3462	6	1624	52955
Luotolax	TUT	AHOW	FA 13/12/1813	19.66	2849	3449	17		
Pena Blanca Spring	UM	AUB	FA 02/08/1946	17.53	2971	2971	0		
Aubres	HUB	AUB	FA 14/09/1836	9.66	2760	3331	17		
Cumberland falls	IGGL	AUB	FA 09/04/1919	14.9	3041	3725	18	2593	78862
Norton County	HUB	AUB	FA 18/02/1948	59.5	2861	3839	25		
Karoonda	HUB	CK5	FA 25/11/1930	14.62	2867	4061	29	4607	132062
Murchison	HUB	CM2	FA 28/09/1969	40.4	2335	3156	26	1021	23836
Ornans	HUB	CO3.3	FA 11/07/1868	8.05	2597	4237	39		
Renazzo	NHMS	CR2	FA 15/01/1824	22.89	3093	3366	8	11004	340370
Allende	TIGT	CV3.2	FA 08/02/1969	21.3	2958	4532	35		
Allende	TIGT	CV3.2	FA 08/02/1969	11.18	2430	5884	59		
Allende	PO	CV3.2	FA 08/02/1969	26.31	2956	3869	24		
Allende	TIGT	CV3.2	FA 08/02/1969	46.77	2960	4032	27		
Allende	PO	CV3.2	FA 08/02/1969	51.5	3121	3787	18		
Allende	PO	CV3.2	FA 08/02/1969	7.85	2804				
Indarch	NHMS	EH4	FA 07/04/1891	41.6	3617	3888	7	24762	895749
Pillistfer	HUB	EL6	FA 08/08/1868	17.42	3629			57483	2086157
Tysnes 1	GMO	H4	FA 20/05/1884	38.7	3225	3617	11	6092	196455
Kashin	VUV	H4	FA 27/02/1918	33.08	3243	3986	19	22955	744457
Jilin	NHMS	H5	FA 08/04/1976	73.4	3398	3925	13	21487	730156
Hessle	GMO	H5	FA 01/01/1869	23.84	3096			17381	538144
Hessle	NHMS	H5	FA 01/01/1869	60.18	3201	3785	15	15738	503769
Forest City	IGGL	H5	FA 02/05/1890	149.7	3426			24642	844137
Werchne Tschirskaja	NHMS	H5	FA 12/11/1843	43.6	3433	3928	13	21510	738438
Pultusk	VUV	H5	FA 30/01/1868	26.5	3487	4206	17	24579	857037
Cornesti	EUB	H5	FA 31/03/1875	20.2	3607			22449	809754
Madaras	EUB	L3.7	FA 04/09/1852	65	2642			1399	36957
Nikolskoe	HUB	L4	FA 06/03/1954	39.94	2959	3840	23	6845	202497
Saratov	VUV	L4	FA 06/09/1918	186.2	3098			7005	217017
Saratov	PO	L4	FA 06/09/1918	20.2	3061	3885	21	9365	286626
Hökmark	NHMS	L4	FA 09/06/1954	78.2	3491	3724	6	9551	333439
Tennasilm	HUB	L4	FA 28/06/1872	45.2	3324	3863	14	5838	194032
Farmington	UM	L5	FA 25/06/1890	16.24	3383	3314		6234	210907
Jhung	GMO	L5	FA 06/1873	24.51	3183	3604	12	9844	313360
Ausson	TUT	L5	FA 09/12/1858	10.2	3290	3923	16	6910	227365
Homestead	GMO	L5	FA 12/02/1875	79	3511			10897	382592
Grefsheim	GMO	L5	FA 25/01/1976	17.95	3520	3387		10230	360072
Buschhof	NHMS	L6	FA 02/06/1863	29.3	3368	3617	7	3946	132890

Bruderheim	UM	L6	FA 04/04/1960	12.51	3381	3381	0	7261	245515
Girgenti	NHMS	L6	FA 10/02/1853	39	3362	3786	11	9172	308385
Oteroy 1	GMO	L6	FA 15/10/1928	23.17	3131	3511	11	5755	180204
Oteroy 2	GMO	L6	FA 15/10/1928	45.33	3309	3656	9	5699	188559
Žemaitkiemio	VUV	L6	FA 1933	11.56	3211	3853	17	7379	236939
Žemaitkiemio	VUV	L6	FA 1933	9.66	3331	3715	10	7813	260249
Žemaitkiemio	VUV	L6	FA 1933	532.6	3302			9975	329360
Zabrodje	VUV	L6	FA 22/09/1893	28.1	3306	3958	16	11585	382983
Zabrodje	VUV	L6	FA 22/09/1893	18.18	3367	3868	13	11003	370444
Zabrodje	IGGL	L6	FA 22/09/1893	32.08	3307	3865	14	11107	367317
Ski	GMO	L6	FA 27/12/1848	610.4	3283			8982	294917
New Concord	VUV	L6	FA 01/05/1860	190.9	3344			9392	314047
Mocs	EUB	L6	FA 03/02/1882	40.9	3195			5957	190355
Lundsgard 1	NHMS	L6	FA 03/04/1889	35.1	3311	3052		8060	266898
Lundsgard 2	NHMS	L6	FA 03/04/1889	66.3	3282			7981	261957
Oesel	NHMS	L6	FA 11/05/1855	49.6	3179	3906	19	4940	157059
Bachmut	NHMS	L6	FA 15/02/1814	42.4	3262	3820	15	5275	172037
Alfianello	GMO	L6	FA 16/02/1883	208.8	2519			9918	249804
Alfianello 1	NHMS	L6	FA 16/02/1883	129.2	3263			8600	280584
Aleppo	NHMS	L6	FA 1873	58.7	3298	3473	5	5718	188571
Žemaitkiemio	VUV	L6	FA 1933	722.2	2951			9941	293392
Leedey	UM	L6	FA 25/10/1943	8.12	3383	3007		7864	266056
Ski	GMO	L6	FA 27/12/1848	37.3	3216	3693	13	7758	249455
Alfianello 2	NHMS	L6	FA 16/02/1883	11.8	3189	3371	5	4065	129648
Knyahinya	GSHB	L/LL5	FA 09/06/1866	48.2	3324				
Knyahinya	EUB	L/LL5	FA 09/06/1866	39.6	3385			4203	142245
Knyahinya	EUB	L/LL5	FA 09/06/1866	65.5	3394			5187	176042
Knyahinya	EUB	L/LL5	FA 09/06/1866	43.3	3331			5054	168336
Holbrook	VUV	L/LL6	FA 19/07/1912	190.6	3231			5090	164447
Holbrook	GMO	L/LL6	FA 19/07/1912	15.77	3092	3755	18	4049	125200
Olivenza	NHMS	LL5	FA 19/06/1924	26.62	3025	3549	15		
Parambu	UM	LL5	FA 24/07/1967	5.29	3306				
Rumuruti	HUB	R3-6	FA 28/01/1934	48.8	3413	3725	8		
Millbillillie	VUV	AEUC	FA 10/1960	31.96	2854				
Pollen	GMO	CM2	FA 06/04/1942	92.9	2266			535	12120
Mighei	HUB	CM2	FA18/06/1889	18.7	1870	3016	38		
Lance	HUB	CO3.4	FA 23/07/1872	61.9	3346	3537	5	2092	70002
Lance	NHMS	CO3.4	FA 23/07/1872	14.7	2882	2882	0	1704	49116
Kaba	GSHB	CV3.0	FA 15/04/1857	3.7	3364			20625	693766
Kaba	GSHB	CV3.0	FA 15/04/1857	4.1	6833			24766	1692356
Ekeby	NHMS	H4	FA 05/04/1939	9.92	3100	3968	22	27137	841254
Lixna	NHMS	H4	FA 12/07/1820	42.6	3550	3944	10	27183	965010
Tysnes 2	GMO	H4	FA 20/05/1884	20.56	3607	3370		12306	443872
Wiluna	UM	H5	FA 02/09/1967	13.59	3576	3883	8	28290	1011737
Limerick	NHMS	H5	FA 10/09/1813	15.8	3591	3098		19713	707859
Zhovtnevyi	UM	H5	FA 10/10/1938	7.41	3368	3222		13227	445501
Juangcheng	PO	H5	FA 15/02/1997	17.93	3898	3815		23793	927397
Hedeskoga	NHMS	H5	FA 20/04/1922	31.7	3484	3819	9	27843	969930
Pultusk	PO	H5	FA 30/01/1868	110.4	3550			28354	1006510
Pultusk	PO	H5	FA 30/01/1868	22.6	3705	4036	8	19185	710796
Charsonville	NHMS	H6	FA 23/10/1810	34.73	3508	3902	10	35072	1230349
Trysil	GMO	L/LL6	FA 21/06/1927	371.1	3389			10954	371247
Hallingeberg	NHMS	L3	FA 01/02/1944	15.92	3122	3317	6	4235	132204

Madaras	NHMS	L3.7	FA 04/09/1852	21.37	3238			5177	167629
Mount Tazerzait	PO	L5	FA 21/08/1991	12.9	3000	4031	26	6927	207800
Mbale	PO	L5/6	FA 14/08/1992	15.33	3407	3739	9	9330	317846
Mocs	EUB	L6	FA 03/02/1882	33.8	3189			8693	277193
Mocs	GSHB	L6	FA 03/02/1882	14.3	3488			7165	249909
Bori	NHMS	L6	FA 09/05/1894	48.8	3297	3697	11	7908	260736
Marion (Iowa)	GMO	L6	FA 25/02/1847	21.99	3282	3727	12	4841	158895
Leedey	NHMS	L6	FA 25/11/1943	107.5	3359	3595	7	6676	224274
Zhigailovka (Kharkov)	TUT	L6 (LL6)	FA 12/10/1787	34.22	3457	4688	26	10732	370963
Sena	HMNHB	H4	FA 17/10/1773	94.4	3396			26076	885468
Beaver Creek	NHMS	H4	FA 26/05/1893	45.3	3283	3872	15	17957	589446
Nuevo Mercurio	UM	H5	FA 15/15/1978	25.1	3218	3922	18	26408	849803
Mjelleim	GMO	H5	FA 24/01/1898	99.3	3534			15837	559662
Timochin	HMNHB	H5	FA 25/03/1807	107.8	3358			25425	853841
Ställdalen	GMO	H5	FA 28/06/1876	115.8	3700			32449	1200513
Ställdalen	NHMS	H5	FA 28/06/1876	53.3	3601	3701	3	36633	1319268
Bialystok	NHMS	AHOW	FA 05/10/1827	43.85	3297	3716	11	7546	248792
Mocs	HMNHB	L6	FA 03/02/1882	68	3350			6793	227559
Mocs	HMNHB	L6	FA 03/02/1882	57.2	3467	3667	5	6704	232393
Mocs	HMNHB	L6	FA 03/02/1882	36.5	3288	3650	10	6680	219647
Dandapur	HMNHB	L6	FA 03/02/1882	14.6	3395			2932	99544
Gambat	HMNHB	L6	FA 15/09/1897	90.4	3194			7726	246782
Aleppo	HMNHB	L6	FA 1873	446	3374			6084	205245
Marion (Iowa)	NHMS	L6	FA 25/02/1847	58.1	3458	3748	8	4139	143129
Dhurmsala	HMNHB	LL6	FA 14/07/1860	149.4	3458			34596	1196433
St. Michel	TUT	L6	FA 12/07/1910	62.2	3475	3616	4		
Camel Donga	VUV	AEUC	FI 01/1984	36.62	2839	3130	9	1561	44326
Camel Donga	PO	AEUC	FI 01/1984	8.3	2594	3609	28		
Reggane	PO	H4	FI 02/04/1989	10.34	3830	3693		12871	492903
Cachari	IGGL	AEUC	FI 05/1916	121.9	2916				
Barratta	VUV	L3.8	FI	233.4	3412			13346	455400
Waconda	IGGL	L6	FI 1873	88.6	3153			6896	217431
Estacado	PO	H6	FI 1883	8.8	3259	3826	15	28214	919560
Estacado	GMO	H6	FI 1883	51.76		3671			
Beenham	UM	L5	FI 1937	8	3333	3200		5773	192442
Mount Egerton	HUB	MES (AUB)	FI 1941	14.76	3514	3433		1625	57107
Mulberry Draw	UM	L5	FI 1963	23.74	3391	3441	1	3827	129806
Tsarev	PO	L5	FI 1968	48.4	3667	3667	0	6456	236712
ALH 76001	GMO	L6	FI 1976	116.7	3278			6343	207932
Julesburg	HUB	L3.6	FI 1983	33.98	3503	3818	8	8659	303317
Owasco	VUV	L6	FI 1984	18.64	3159	3452	8		
Oliver	UM	L6	FI 1984	12.54	3389	3389	0	3018	102287
Acfer 90087	UM	CR2	FI 1990	23.7	3292	4086	19	10830	356486
Hughes 021	HUB	L3.6	FI 1991	4.89	3493	3944	11		
DaG 067	UM	CO3	FI 1995	31.88	3321	3542	6	2753	91420
DaG 391	UM	AEUC	FI 1997	18.09	2966	3289	10		
DaG 380	UM	AEUC	FI 1997	18.22	3037	3644	17		
Sahara 97193	HUB	L3.9	FI 1997	28.5	3701	3851	4	4402	162926
Dhofar 055	UM	AEUC	FI 1999	13.62	2961	3322	11		
Sayh al Uhaymir 281	HUB	EH3	FI 2001	12.96	2817	3600	22	6553	184611
Svartekari	GMO	H5	FI 2001	711.5	3552			39344	1397571
Nova 004	UM	H5	FI 2002	42.06	3448	3894	11	27167	936606
NWA 3094	HUB	L6 imp. melted	FI 2003	31.7	3446	3774	9	13235	456035

NWA 3080	HUB	L6 imp. melted	FI 2003	18.5	3627	3627	0	11711	424796
NWA 3050	HUB	L6 imp. melted	FI 2003	14.1	3439	3811	10	5607	192823
NWA 3057	HUB	L6 imp. melted	FI 2003	26.5	3581	3897	8	17587	629817
Hanno 04 (NWA)	HUB	L4 imp. melted	FI 2004	13.59	3398	3883	13	8334	283160
Fortuna	HUB	AWIN	FI 27/05/1998	9.52	3662	4533	19	20682	757272
Dhofar 125	HUB	ACAP	FI 2000	29.04	3585	3676	2	9334	334645
Kenna	HUB	AURE	FI 1972	31.3	4118	3598		3899	160568
Hammadah al Hamra 126	HUB	AURE	FI 1972	21.19	3451	3418		3806	131364

Table 2:

True susceptibility		Ellipsoid axis ratio		Demag. factors		Apparent susceptibility along a		Apparent susceptibility along b, c	
κ_{mass} (10^{-8} m^3/kg)	κ_{bulk} (10^{-6}SI)	a	b, c	N_a	$N_{b,c}$	κ_{bulk} (10^{-6}SI)	difference (%)	κ_{bulk} (10^{-6}SI)	difference (%)
500	16000	4	1	0.08	0.46	15980	0.1	15883	0.7
5000	160000			0.08	0.46	157978	1.3	149031	6.9
50000	1600000			0.08	0.46	1418440	11.3	921659	42.4
500000	16000000			0.08	0.46	7017544	56.1	1913876	88.0
500	16000	2	1	0.18	0.41	15954	0.3	15896	0.7
5000	160000			0.18	0.41	155521	2.8	150150	6.2
50000	1600000			0.18	0.41	1242236	22.4	966184	39.6
500000	16000000			0.18	0.41	4123711	74.2	2116402	86.8
500	16000	1	1	0.33	0.33	15916	0.5	15916	0.5
5000	160000			0.33	0.33	151976	5.0	151976	5.0
50000	1600000			0.33	0.33	1047120	34.6	1047120	34.6
500000	16000000			0.33	0.33	2547771	84.1	2547771	84.1
500	16000	0.7	1	0.44	0.28	15888	0.7	15929	0.4
5000	160000			0.44	0.28	149477	6.6	153139	4.3
50000	1600000			0.44	0.28	938967	41.3	1104972	30.9
500000	16000000			0.44	0.28	1990050	87.6	2919708	81.8
500	16000	0.5	1	0.52	0.24	15868	0.8	15939	0.4
5000	160000			0.52	0.24	147710	7.7	154083	3.7
50000	1600000			0.52	0.24	873362	45.4	1156069	27.7
500000	16000000			0.52	0.24	1716738	89.3	3305785	79.3
500	16000	0.3	1	0.66	0.17	15833	1.0	15957	0.3
5000	160000			0.66	0.17	144718	9.6	155763	2.6
50000	1600000			0.66	0.17	778210	51.4	1257862	21.4
500000	16000000			0.66	0.17	1384083	91.3	4301075	73.1

Figure 1:

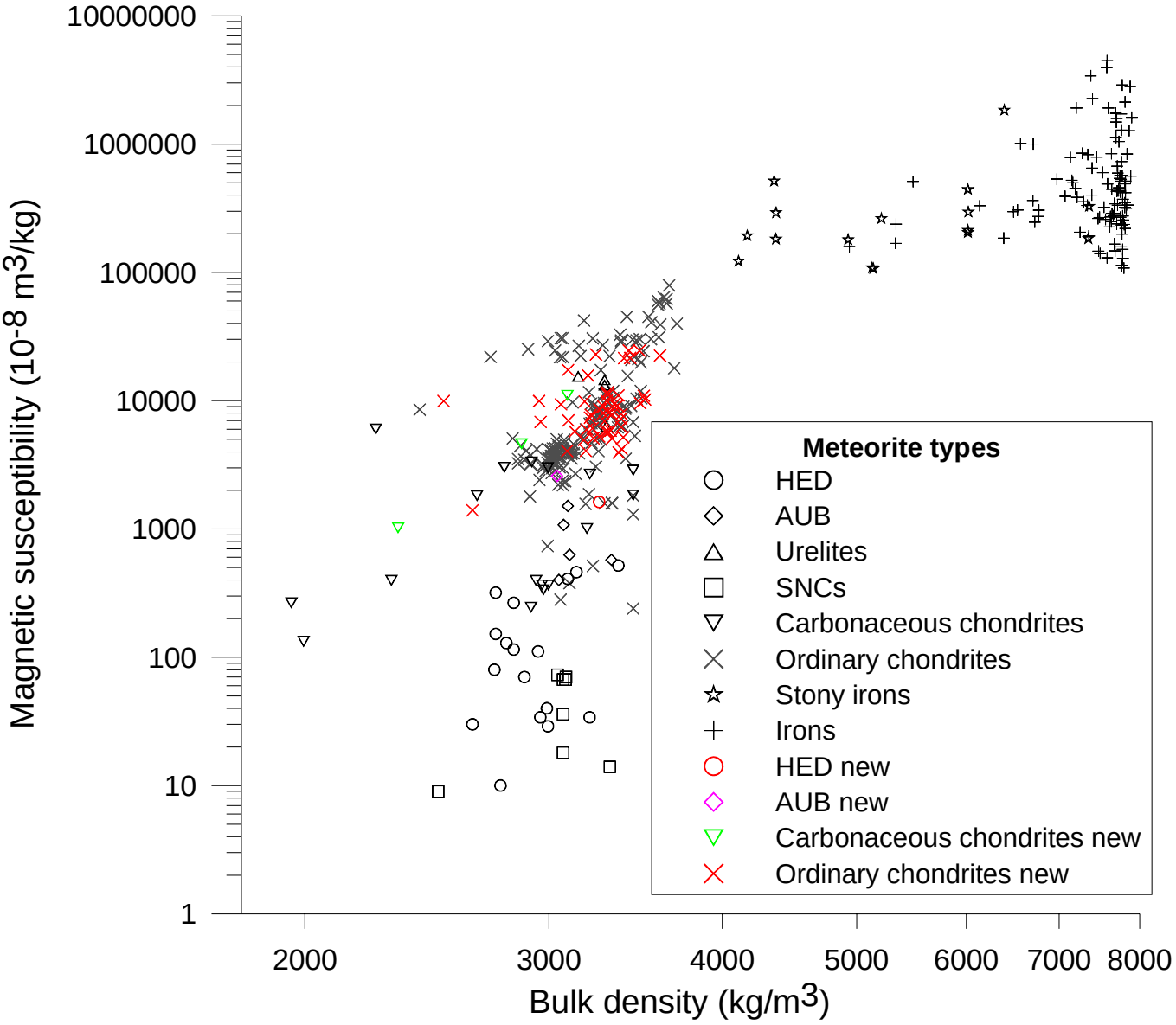
Magnetic susceptibility (10-8 m3/kg)
10000000
1000000
100000
10000
1000
100
10
1
2000
3000
4000
5000
6000
7000
8000
Bulk density (kg/m3)
Meteorite types
HED
AUB
Urelites
SNCs
Carbonaceous chondrites
Ordinary chondrites
Stony irons
Irons
HED new
AUB new
Carbonaceous chondrites new
Ordinary chondrites new

Figure 2:

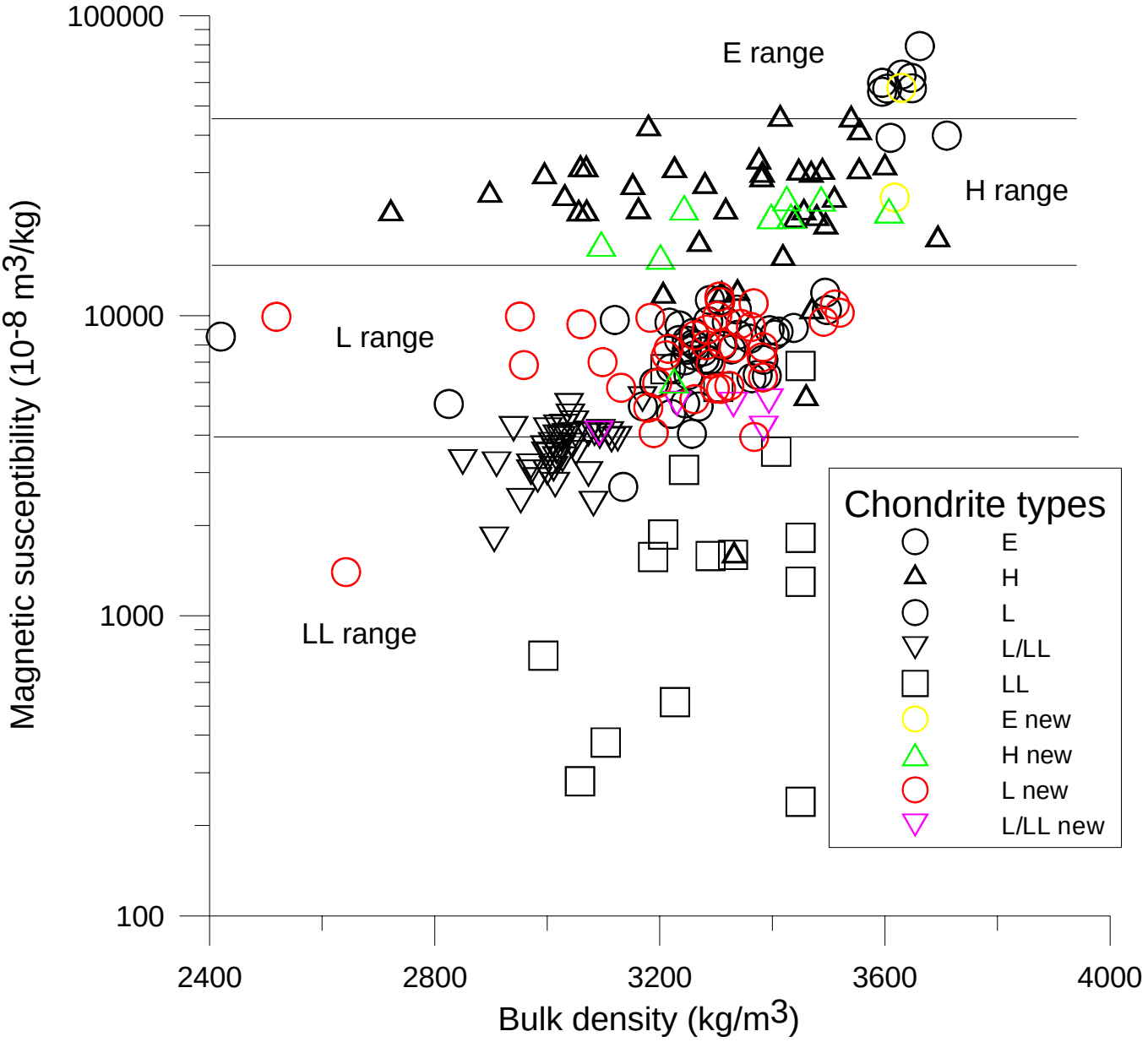
100000
10000
1000
100
Magnetic susceptibility (10-8 m3/kg)
2400
2800
3200
3600
4000
Bulk density (kg/m3)
E range
H range
L range
LL range
Chondrite types
E
H
L
L/LL
LL
E new
H new
L new
L/LL new

Figure 3:

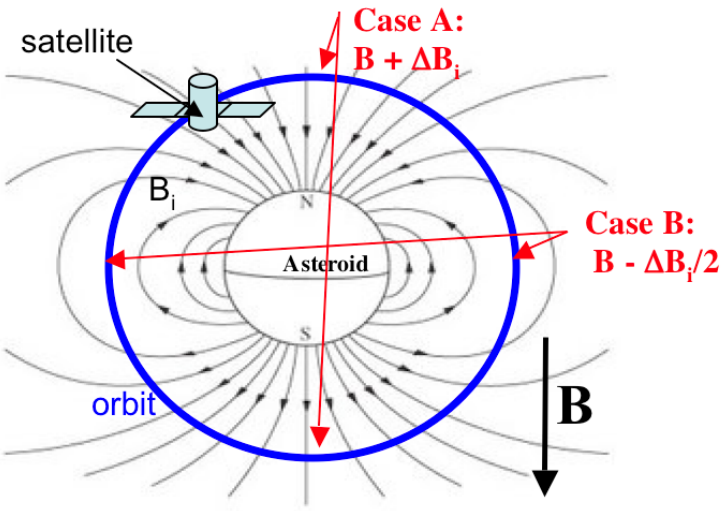

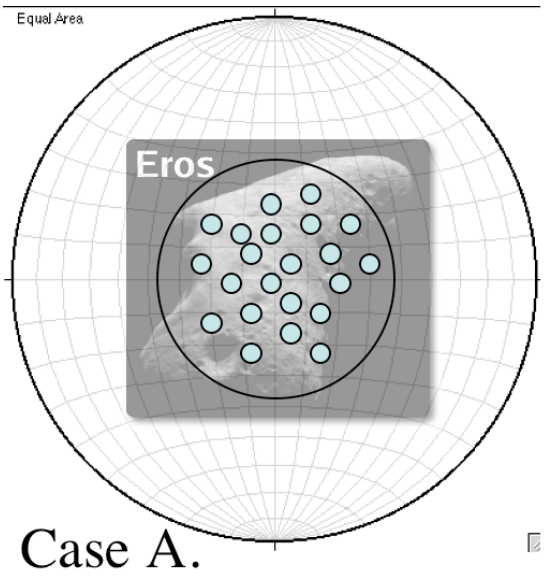

Case A.

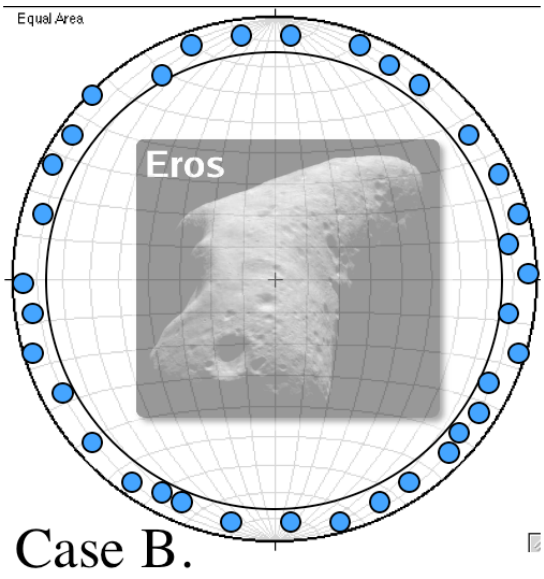

Case B.